Chemical Science

ROYAL SOCIETY OF CHEMISTRY

EDGE ARTICLE

View Article Online
View Journal | View Issue

Cite this: *Chem. Sci.*, 2025, **16**, 1809

All publication charges for this article have been paid for by the Royal Society of Chemistry

Phosphite mediated molecular editing *via* switch to *meta*-C–H alkylation of isoquinolines: emergence of a distinct photochemical [1,3] N to C rearrangement†

Soniya Rani, ‡[ab] Anuj Kumar Ray,‡[c] Devendra Kumar Dewangan, ‡[ab] Nita Aruna Ramchandra Patil,[a] M Aarthika, [ab] Ankan Paul *[c] and Pradip Maity *[ab]

The isoquinoline core is present in one of the largest subsets of bioactive natural products. The multifunctional isoquinoline core exerts diverse bioactivity, resulting in the development of numerous isoquinoline-based drugs and molecules that are currently under clinical trials. We developed a new approach for phosphite-mediated [1,2] alkyl migration for an overall *ortho*-C–H alkylation *via* *N*-alkylation of isoquinoline. Tuning the phosphite-mediated protocol to switch the site selectivity would expedite direct and diverse multi-C–H bond functionalization. We report a new approach starting with a simple *N*-alkylation of isoquinoline with sterically and electronically diverse alkyl bromides for their phosphite-mediated photochemical [1,3] N to C rearrangement followed by a rearomatization sequence that leads to *meta*-C–H (C4) alkylation. Combined experimental and computational studies unveiled the emergence of an unprecedented C–N bond cleavage pathway from the singlet excited state of the enamine-type intermediate. Our radical bond-cleavage pathway favors substituted alkyl group migration that complements the recently successful *meta*-alkylation methods with smaller and more reactive electrophiles. This switch in site selectivity *via* tuning the phosphite-mediated protocol resulted in sequential C–H difunctionalization of isoquinoline including regiodivergent *ortho*, *meta*-dialkylations of isoquinolines.

Received 21st October 2024
Accepted 9th December 2024

DOI: 10.1039/d4sc07127a

rsc.li/chemical-science

Introduction

Isoquinoline is an important structural core in a diverse array of natural products (over 2500) and drugs currently in use or under clinical trials.[1] The synthesis of multi-functionalized isoquinoline gained significant focus due to their prevalence in pharmaceuticals,[2a] agrochemicals,[2b] chiral ligands,[2c] and materials.[2d] Direct molecular editing of isoquinoline C–H bonds through consecutive selective C–H functionalization can provide access to diverse analogs valuable in pharmaceuticals.[3] Substitution at each carbon of the isoquinoline core is prevalent, including *meta*-functionalized bioactive compounds with substituted alkyl groups (Fig. 1A).[4] Among different C–H bonds, *ortho*- and *para*-alkylations were achieved successfully with a broad range of electronically and sterically diverse substituents.[5] However, *meta*-C–H alkylation remained a formidable challenge due to its inertness towards both electrophilic and nucleophilic reagents. As a result, most of the isoquinoline natural products containing *meta*-alkyl substitution were synthesized from their alkyl substituted acyclic precursors.[4,6]

In a more direct approach, Minter and Re in 1988 showed a one-pot multi-step operation for effective *meta*-C–H alkylation of isoquinolines with aldehydes (Fig. 1B).[7a] This strategy is based on reductive hydroboration, followed by electrophilic functionalization of the resulting enamine, and finally, dehydration–tautomerization for the overall *meta*-alkylation. The reaction was shown to work only with aldehydes, limiting it to the installation of primary alkyl groups. In 2017, Du, Zhang, and co-workers reported a similar strategy *via* initial hydrogenation rather than hydroboration.[7b] Catalytic hydrogenation by formic acid resulted in less waste-generation, but it remained limited to primary alkylation.

In 2022, the Wang group developed an improved Lewis acid catalyzed reductive hydroboration to enamine and its electrophilic functionalization at *meta*-C–H. The catalyst activation led to successful reaction with activated ketones and imines, along

[a]*Organic Chemistry Division, CSIR-National Chemical Laboratory (CSIR-NCL), Pune 411 008, India. E-mail: p.maity@ncl.res.in*

[b]*Academy of Scientific and Innovative Research (AcSIR), Ghaziabad 201002, India*

[c]*School of Chemical Sciences, Indian Association for the Cultivation of Science, Kolkata 700032, India. E-mail: rcap@iacs.res.in*

† Electronic supplementary information (ESI) available. See DOI: https://doi.org/10.1039/d4sc07127a

‡ S. R., A. K. R. and D. K. D. contributed equally to this work.

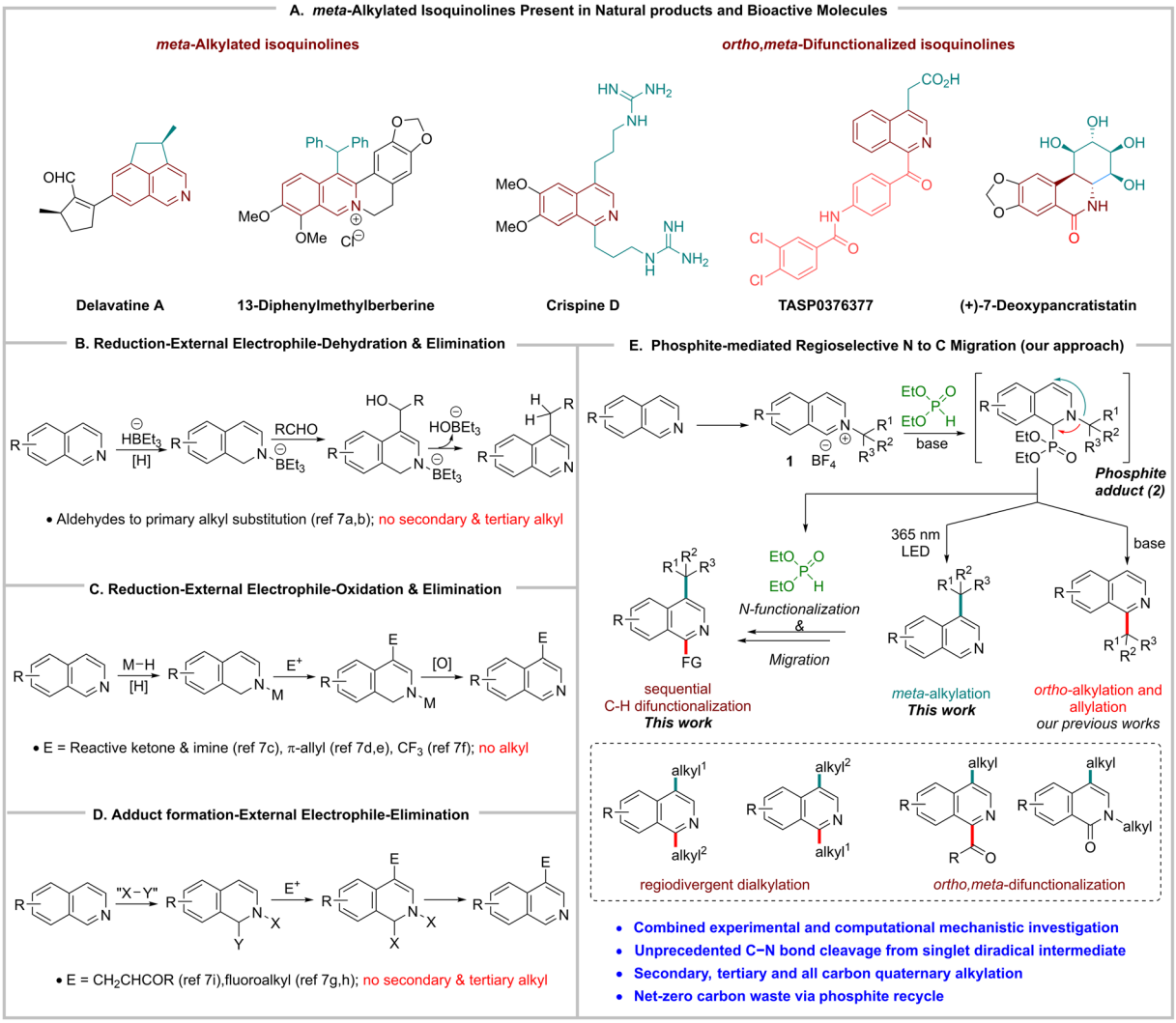

Fig. 1 (A) Natural products and biologically active compounds with *meta*-alkylated isoquinoline core. (B–D) Reported strategies for *meta*-C–H alkylations of isoquinolines. (E) *N*-Functionalization of isoquinoline and phosphite-mediated regioselective N to C migration.

with aldehydes. Additionally, a second equivalent of electrophiles oxidized the C3 functionalized enamine intermediate for an overall *meta*-C–H amino and hydroxyl alkylation (Fig. 1C).[7c] In 2023, the Wang group followed up with an asymmetric *meta*-allylation with reactive chiral iridium and palladium π-allyl electrophiles.[7d,e] In 2022, the Kuninobu group utilized a similar approach with silane as the reductant for *meta*-selective trifluoromethylation.[7f] In these redox approaches, both pre-reduction and post-oxidation steps require extra catalysts and stoichiometric reagents, leading to waste generation. Importantly, activated electrophiles were required for successful *meta*-functionalization, and no reaction was reported with simple alkyl electrophiles such as alkyl halides.

In 2022, Studer and co-workers reported a *meta*-selective radical fluoroalkylation of azaarenes *via* a redox neutral reaction sequence.[7g,h] In 2023, the Donohoe group developed an excess benzoic acid-mediated one-pot *meta*-alkylation of isoquinolines with unsubstituted vinyl ketones, leading to primary alkyl group installation.[7i] These elegant methods avoid the reduction and oxidation of azaarenes for their *meta*-C–H alkylation. However, they are limited to strong alkylating electrophiles only, owing to a similarly reactive enamine intermediate developed *via* reduction.[7a–f] The requirement of stoichiometric reagents to form dearomatized adducts and their removal after alkylation led to waste generation (Fig. 1D). A direct and waste-free *meta*-alkylation with unactivated and sterically demanding alkyl halides remains elusive.

One of our research programs focuses on the facile synthesis of *N*-functionalized pyridinium salts for their phosphite-catalyzed migration to the ring carbons (Fig. 1E).[8] The allyl and alkyl groups on pyridine nitrogen successfully migrated to the C2 position for overall *ortho*-allylation and alkylation.[8a,b] A switch in site selectivity to regiodivergent C–H alkylation from the same *N*-alkylpyridinium salts under tunable reaction conditions would be highly advantageous for diversity-oriented synthesis. Regiodivergent switch between *ortho*- and *para*-positions has been achieved due to their similar electrophilic reactivity pattern. The switch is usually accomplished by taking

advantage of the nitrogen coordination to either direct the nucleophile to the *ortho*-position, or sterically block the *ortho*-position with bulky nitrogen-coordinating additives.[9] However, switching the same functional group between *ortho*-/*para*- and *meta*-C–H bonds is very challenging due to their differential reactivity.

Transition metal catalyzed *ortho*-/*para*- and *meta*-C–H activation followed by borylation, arylation, and alkenylations of azaarenes was established recently. The switch in selectivity was achieved *via* different catalysts with precisely designed ligands.[3,10] A more attractive electrochemical carboxylation was recently reported by Yu, Lin, and co-workers, where the switch from *meta*- to *para*-carboxylation was achieved simply by using either divided or undivided cells.[11] In 2023, the Studer group reported an elegant switch to *para*-C–H alkylation from their previous *meta*-C–H fluoroalkylation *via* a simple change in the pH of the reaction. However, *para*-alkylation needs a nucleophilic alkyl radical coupling partner, while *meta*-fluoroalkylation works with electronically opposite electrophilic radicals.[7h,12] To the best of our knowledge, a switch between *ortho*- and *meta*-positions by electronically similar alkyl groups has not been reported.

Herein, we report that direct photochemical irradiation under a 365 nm LED to the phosphite adduct (**2**) of *N*-alkyl isoquinolinium salt (**1**) resulted in *meta*-C–H alkylation. The unique feature of our approach is the dual role of the functional group on nitrogen to act as a nitrogen activator to facilitate phosphite adduct (**2**) formation, followed by its migration from nitrogen to ring carbon (Fig. 1E). The migration from nitrogen deactivates it, which triggers the *in situ* phosphite elimination for an overall C–H functionalization. The recovery and reuse of phosphite after work-up make the overall transformation net-zero in carbon waste. The one-pot method starts with either bench-stable *N*-alkyl isoquinolinium salt **1** or directly from isoquinoline and alkyl halides. Experimental and computational evidence was presented for a plausible mechanism for this unprecedented *meta*-C–H alkylation with primary, secondary, and tertiary alkyl groups. Furthermore, consecutive functionalization on isoquinoline nitrogen and its migration to the ring carbons under the same phosphite-mediated tunable reaction conditions allow for selective and regioisomeric *ortho*, *meta*-di-C–H functionalization with chemically equivalent alkyl halides. The utility of phosphite-mediated methods *via* *N*-functionalization was further demonstrated for the derivatization of *meta*-alkylated products.

Results and discussion

N-Alkylation of isoquinoline

First, we screened conditions for a direct alkylation on isoquinoline nitrogen. A simple solvent-free mixing of isoquinoline with primary, secondary, and tertiary alkyl halides at ambient to moderate temperature led to the corresponding *N*-alkyl isoquinolinium halide salt formation with good to excellent yields.[13] Some of the halide salts are hygroscopic in nature and form color impurities when stored for months. Literature-modified ion exchange methods were employed to the corresponding tetrafluoroborate salts that are not hygroscopic and are bench stable for years without degradation. A direct tetrafluoroborate salt formation was also achieved *via* stirring isoquinoline and corresponding alkyl halide in acetone with six equivalents of sodium tetrafluoroborate as an additive.[14]

Development of phosphite mediated photochemical *meta*-alkylation

We envisioned that the phosphite-adduct **2** of *N*-isoquinolinium salt could be perceived as an *N*-alkylated aryl-conjugated enamine or amine-conjugated styrene derivative. The [1,3] O-to-C rearrangement of an O-alkylated aryl-conjugated enol is well established *via* both ionic and radical pathways.[15] The corresponding aza-version with N-to-C migration is rare, with only one thermal migration known to occur from l,4-dialkyl-l,4-dihydropyrazines *via* stereoinversion.[16] We plan to explore a similar N-to-C [1,3] alkyl shift, owing to our previous success with other phosphite-mediated aza-migrations around azaarenes.[8a,b] Thermally heating the phosphite adduct **2** did not result in any migration product.

Next, we explored the possibility of photochemically exciting the amine-conjugated styrene part of the adduct **2** for a possible photochemical aza-[1,3] migration. Our photophysical studies of adduct **2** showed that it could be excited with 365 nm light. A fluorescence emission study with excitations at different wavelengths established better absorption at 365 nm with the highest emission (see ESI†). Therefore, we explored a one-pot phosphite addition, followed by its direct excitation for aza-[1,3] shift and subsequent base-mediated phosphite elimination for the *meta*-alkylation of isoquinoline (Table 1). Delightfully, the one-pot reaction sequence with the stoichiometric phosphite additive in *p*-xylene with four equivalents of

Table 1 Optimization study of *meta*-C–H alkylation

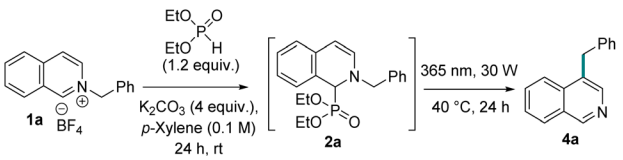

Entry[a]	Deviation from standard conditions[a]	Yield[b] (%)
1	None	60
2[c]	One-pot with **1a**-bromide	58
3	50 mol% phosphite	35
4	Other solvents	5–44
5	3 equiv. of K_2CO_3	54
6	5 equiv. of K_2CO_3	60
7	Other bases	10–50
8	$\lambda_{max} = 320$ nm	<5
9	$\lambda_{max} = 380$ nm	40
10	$\lambda_{max} = 395$ nm	29
11	$\lambda_{max} = 365$ nm, 18 W	34
12	No light	n.d.
13[d]	No base	<5

[a] 0.2 mmol scale. [b] Isolated yield. [c] One-pot *N*-alkylation and migration to the *meta*-position. [d] For the second step. n.d. – not detected.

potassium carbonate as a base led to the *meta*-benzyl isoquinoline in 60% yield with complete regioselectivity (entry 1). Starting with the *N*-benzylation of isoquinoline and its one-pot migration also yielded the product with comparable efficiency (entry 2). Catalytic amounts of phosphite resulted in lower yield with no trace of unreacted starting material or intermediate (**2a**) in the crude reaction mass (entry 3). On the other hand, phosphite was regenerated quantitatively. Therefore, we chose to proceed with stoichiometric phosphite to complete **2a** formation under darkness, followed by its photochemical *meta*-alkylation. Diethylphosphite can be separated from the product and other impurities *via* a simple aqueous work-up protocol (see ESI†). Reaction in other solvents also formed the product, but the *p*-xylene remains the best (entry 4, see ESI for details†). Changing base equivalents or other bases led to lower yields (entries 5–7). As anticipated from our photophysical studies, different light sources with higher and lower frequencies led to a drop in reaction efficiencies (entries 8–10). The light intensity is important, with low power light (18 W) leads to lower yield (entry 11). No *meta*-benzyl isoquinoline formation was observed without light, and a trace amount of product formation was observed without base (entries 12 and 13).

Substrate scope

Under the optimized reaction conditions, we screened the substrate scope (Fig. 2), focusing on the migrating alkyl group first. A chloro substituent at *ortho*-, *meta*-, and *para*-to the phenyl ring (**4b–d**) worked better than the unsubstituted benzyl migrating group. These results indicate that the steric crowd is tolerant around the aryl ring. Other halides at the *meta*-position were equally efficient (**4e–g**). The compatibility of all halides at different positions of the aryl substituents is significant since a transition metal catalyzed *meta*-alkylation could be problematic for these substituents. Both electron-deficient groups such as cyano (**4h**) and ester (**4i**), and electron donating methyl (**4j**) and methoxy (**4k**) were well tolerated at the *meta*-position. The electron-deficient cyano substitution in the *para*-position (**4l**) resulted in good yields. However, the electron-donating methyl group led to a low 24% yield (**4m**). With this trend, we tested other non-phenyl aryl groups on migrating carbon. An electron neutral β-naphthyl (**4n**) and electron-deficient 3- and 4-pyridines gave products (**4o,p**) with good yields, while electron-rich furan (**4q**) and thiophene rings (**4r**) led to lower yields. After the success of a wide variety of substituted benzyl migration, we tested the suitability of non-benzyl groups. An *N*-allyl group on nitrogen (**4s**) was migrated successfully with good yields. The chemoselective reduction of the corresponding *meta*-allyl isoquinoline led to a *meta*-alkylated product (**4t**). A direct *meta*-alkylation *via* *N*-alkylation and migration of alkyl groups, such as methyl and ethyl, failed under our reaction protocol. An ester substitution on migrating alkyl carbon also migrated successfully (**4u**) in 58% yield.

We next examined the scope of our method with substituted isoquinolines. Substitution at the C1 position is not reported for *meta*-C–H alkylation, presumably due to their reduced reactivity towards reduction and nucleophilic addition to form the enamine-type intermediate.[7] Since the phosphite anion is a better nucleophile, we tested our protocol with the 1-methylisoquinoline substrate. Both benzyl and diphenylmethyl salts of 1-methylisoquinoline formed the phosphite adduct smoothly, and led to successful product formation under the photochemical reaction conditions (**4v**, **4w**). Methyl substitution at the C3 position yielded the *meta*-benzylated product (**4x**) successfully under prolonged irradiation. On the fused benzene ring of the isoquinoline, we explored electron-rich substituents due to their prevalence in natural products.[4] Methoxy or dimethoxy substitutions on the fused benzene ring of the isoquinoline successfully yielded the corresponding products with similar efficiencies (**4y,z,aa**). We also tested bromo-substitution on either ring of isoquinoline (C3 and C6), but the corresponding phosphite adduct remained unreactive under the optimized reaction conditions. Longer irradiation led to slow decomposition for both the substrates. We anticipated that a shorter singlet excited state lifetime *via* facile singlet to triplet intersystem crossing in chromophores conjugated with bromides could be the reason for their inertness. These results reinforce our mechanistic hypothesis that the [1,3] migration proceeds *via* a singlet excited state.[17] It is noteworthy to mention that all aryl halides are tolerated when they are not conjugated with the chromophore (**4b–g**).

Many of the bioactive isoquinolines with *meta*-alkyl substitution are tertiary alkyl groups.[4,18] Therefore, we tested our method for the *N*-alkylation and migration of secondary alkyl halides. The more substituted isoquinolinium salt (**1**) from a secondary alkyl halide with alkyl and aryl substitutions led to better yields than the parent benzyl group. A methyl and phenyl substitution on the migrating carbon led to a 66% yield of the tertiary alkylated isoquinoline product (**4ab**). Expectedly, a methyl and electron-poor aryl substitution resulted in slightly better yields (**4ac,ad**). An ethyl instead of methyl as the alkyl substitution is equally efficient (**4ae**). Interestingly, cyclopropyl as the alkyl substitution led to normal cyclopropyl product formation (**4af**) without any detectable ring-opening product. The success of a wide variety of substituents on the migrating carbon makes this method attractive as a general *meta*-C–H alkyl protocol. The better results with sterically demanding substituted alkyl groups complement the known *meta*-C–H alkylation methods where steric crowding led to poor yields or failed reactions.[7] Migration of dibenzylic groups was studied next, which led to the highest 78% yield for diphenyl substitution (**4ag**). Other diarylmethyl groups also worked well to form the triarylmethane products (**4ah,ai**) in good yields. We also tested the alkylation on nitrogen with the α-oxy aryl lactone (phthalide) substituted alkyl group due to their prevalence in natural products.[19] *N*-alkylation with a group containing a heteroatom is tricky due to its instability.[20] A modified *N*-alkylation and photochemical migration protocol with a milder triethylamine base at a lower temperature resulted in the successful migration of this sensitive group with 68% yield (**4aj**). A methyl and ester substituted alkyl also migrates successfully (**4ak**). Finally, we tested the migration of a tertiary alkyl group at the *meta*-C–H position. The dimethylphenyl substituted substrate successfully formed the product (**4al**) with

a 40% yield. Although the yield is lower, a quaternary carbon center formation at *meta*-C–H with an all carbon alkyl group has not been achieved previously. The increase in steric and nucleophilicity of the tertiary alkyl group due to the extra methyl substitution might be the cause of moderate yield with substantial dimerization of the migrating group.

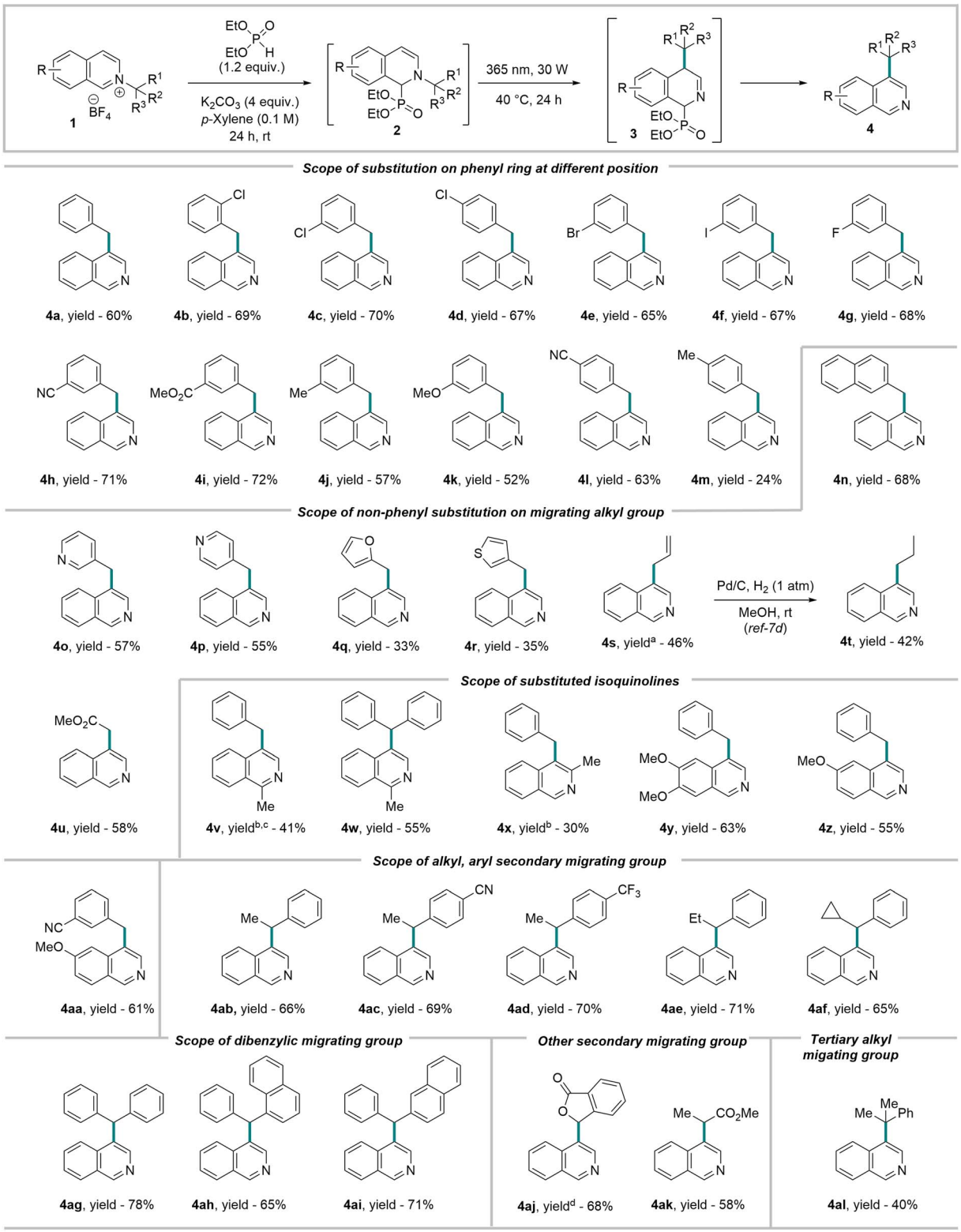

Fig. 2 Substrate scope. All reactions were performed on 0.2 mmol scale. All yields are isolated. [a]Reaction time in the light is 60 h. [b]Reaction time in the light is 72 h. [c]% Conversion is 70. [d]**1aj** (0.2 mmol), diethylphosphite (0.24 mmol), Et_3N (0.3 mmol) and 2.5 ml DCM, 24 h, −40 °C; K_2CO_3 (0.5 mmol), *p*-xylene (0.1 M), 30 W LED (λ_{max} = 365 nm), 24 h, 15 °C.

Mechanistic studies

Although photochemical aza-[1,3] migration is not known, various other photochemical [1,3] migrations are reported to undergo *via* a concerted pericyclic pathway[21] and dissociative mechanism with radical recombination[22] or radical chain propagation.[23] To understand our reaction path, we carefully analyzed our reactions to detect any intermediate and side-products formed in the reaction. In that effort, we found a 5–20% dimer (**5**) of the migrating alkyl group depending on their reactivity. Electron-rich benzyl radicals and tertiary alkyl radicals were more prone to dimerization. The degree of dimerization is inversely correlated with the yields of *meta*-alkylated product formation. This dimer formation suggests a homolytically dissociative mechanism for our *meta*-alkyl migration. We also isolated small amounts (5–10%) of *ortho*-phosphonate isoquinoline (**6**). We presume this might be formed *via* the single electron oxidation of the other radical partner (**R1**) (Fig. 3A). The classical TEMPO trapping experiment led to the benzyl-TEMPO adduct (**7a**), further supporting homolytic C–N dissociation as the reaction initiation step (Fig. 3B). A direct photochemical excitation of the adduct **2** excites it to the singlet state, and therefore, the dissociation from either a singlet or triplet state is feasible. To experimentally distinguish between these two possibilities, we set to attain singlet and triplet excited states selectively to study their reactivity. A triplet quencher like naphthalene diminishes the product formation by only 7%.[24] However, an iridium based triplet photosensitizer with higher triplet energy than the adduct **2** (calculated to be 53.6 kcal mol^{-1}) led to 10% product formation under 450 nm light irradiation (Fig. 3C).[25] No reaction occurred with direct 450 nm light excitation without the iridium photosensitizer. These results indicate a major reaction path from the singlet excited state with a minor triplet state component.

To shed light on the reaction mechanism, we conducted TDDFT and DFT computations with model dimethylphosphite adduct **2a** bearing a benzyl as the migrating group. We truncated the ethyl groups present on the phosphite to methyl groups in order to reduce the computational cost. The first singlet excited state (S_1) was found to be the bright state, and the S_1 optimized intermediate 2_S^* lies at 77.7 kcal mol^{-1} above the adduct **2a** (Fig. 3E). The activation total energy ($\Delta E_0^{\ddagger}$) for the C–N bond dissociation at the S_1 surface was estimated to be +5.7 kcal mol^{-1} above the Franck–Condon geometry on the S_1 surface. The $\Delta E_0^{\ddagger}$ from the S_1 equilibrium was found to be +14.8 kcal mol^{-1}. Alternatively, 2_S^* could undergo inter-system crossing (ISC) to its triplet state T_1 forming intermediate 2_T^*. To check whether ISC is feasible, we computed the spin orbit coupling matrix elements (SOCME) at the CASSCF level including 3 singlets and 2 triplets at S_0, S_1 and T_1 geometries (see ESI for details†). Since, all the spin orbit coupling matrix elements have paltry values (<1 cm^{-1}) the rate for ISC is expected to be significantly slow, making the dissociation at the S_1 surface the favored pathway.[26] This observation is expected according to El-sayed's rule[27] as the photoexcitations involved in **2a** are of only π–π^* nature (see ESI†). In order to obtain further insights into the photoexcited bond dissociation process, we performed relaxed potential energy scans considering the singlet ground state (S_0) and two most important excited states, namely, first excited singlet (S_1) and triplet states (T_1) using DFT/TDDFT (M062X/6-31++G(d,p)) (see ESI for details†). The density functional studies rather suggested a substantial barrier to dissociation on the S_1 surface.

Since the chemical transformation involves a bond breaking scenario under photoexcitation, for obtaining more reliable estimates on energetics proper treatment of static and dynamic electron correlation is needed.[28] Hence, we carried out single point calculations on relevant DFT optimized geometries with strongly contracted n-electron valence state perturbation theory (SC-NEVPT2)[29] (see ESI†). According to the computed NEVPT2 energetics the barriers associated with the desired C–N bond cleavage are similar on both S_1 and T_1 surfaces. The NEVPT2 studies revealed that the TS lies just 4.6 kcal mol^{-1} above the Franck–Condon region on the S_1 excited state surface (see ESI†). Hence, it can be expected that a significant fraction of photo-excited molecules will undergo C–N bond dissociation, while a larger fraction will relax to the S_1 minimum leading to fluorescence (which we experimentally observe). Furthermore, we theoretically studied the congener of **2a** having *p*-CN substitution at the migrating phenyl group (see ESI†), which provides a higher yield of the photoproduct compared to that of **2a** experimentally. It was found that the TS for C–N photo-dissociation lies below the Franck–Condon geometry on the S_1 surface and only 2.6 kcal mol^{-1} above the S_1 minimum. Based on these observations and low computed SOCME values we propose this channel at S_1 to be the dominant pathway for C–N photo-dissociation.

Next, we tried to understand the C–C bond formation mechanism from the bis-radical intermediacy (**R1** & **R2**). Most photochemical [1,3] rearrangements were proposed to form C–X bonds *via* a radical-chain propagation mechanism.[22] However, photoexcited aryl enamines with bicyclic N–O substituted compounds are reported to undergo a [1,3] shift *via* intramolecular radical recombination.[22] For our [1,3] alkyl shift, either the benzyl–benzyl (**R1** & **R2**) radical recombination to intermediate **3**, or a benzyl radical (**R2**) addition to the electron-rich enamine (**2**) for chain propagation could be kinetically challenging (Fig. 3D). Both mechanistic pathways explain poor yields with electron-rich migrating alkyl radicals while better results with electron-deficient ones. We performed a crossover experiment with **1h** and **1z** to gain experimental evidence. The recombination mechanism should predominantly produce only normal products (**4h** and **4z**), provided the concentration of the radicals is low at any point. On the other hand, the chain mechanism would generate all four products, including **4a** and **4aa** (Fig. 3F).[23] The fact that we obtained major normal products with significant cross-products indicates the possibility of both pathways operating at variable degrees. The fact that the radical trapping experiment with TEMPO (Fig. 3B) did not completely shut down the product formation also suggests partial radical recombination *via* solvent-trapped intermediates (**R1** & **R2**).[15b,30] The feasibility of the radical chain propagation path was calculated next. The electrophilic migrating radical **R2** generated *via* C–N bond dissociation can attack another electron-rich

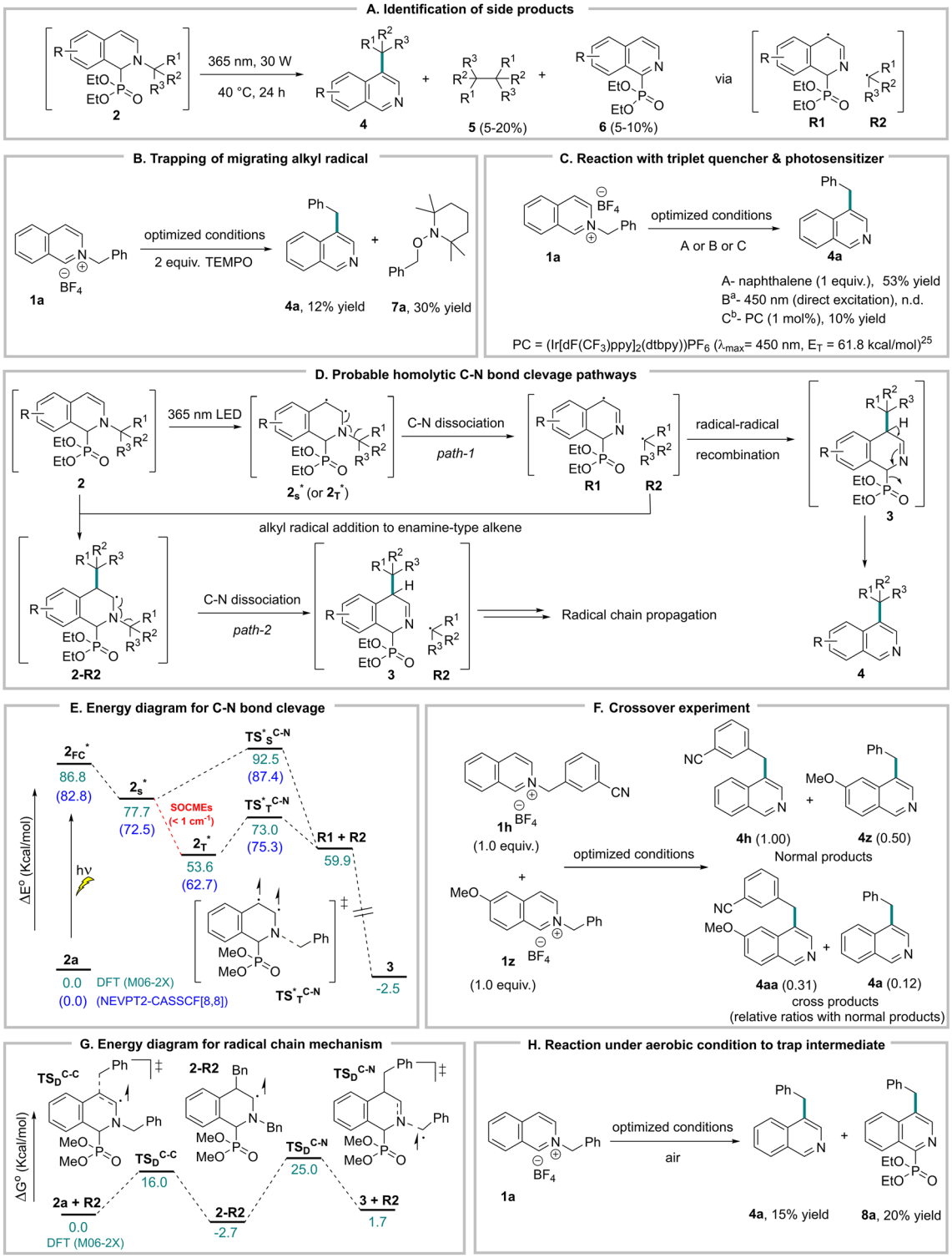

Fig. 3 Mechanistic investigation. All reactions were performed on 0.2 mmol scale. Isolated yields are given. [a]More than 95% intermediate remaining. [b]15% intermediate remaining. n.d. – not detected.

adduct **2a** at the *meta*-position to form intermediate **2-R2**. The activation barrier for such addition is 16.0 kcal mol^{-1} with the benzyl radical. Subsequent N–benzyl bond dissociation would form the aza-[1,3] migrated product (**3**) with another benzyl radical (**R2**) for chain propagation (Fig. 3G). The activation barrier for the C–N bond dissociation from **2-R2** was calculated to be 27.7 kcal mol^{-1}, making it feasible at a reaction temperature of 40 °C.

The final *meta*-alkylation product formation from the aza-[1,3] alkyl shifted intermediate **3** is proposed to undergo *via*

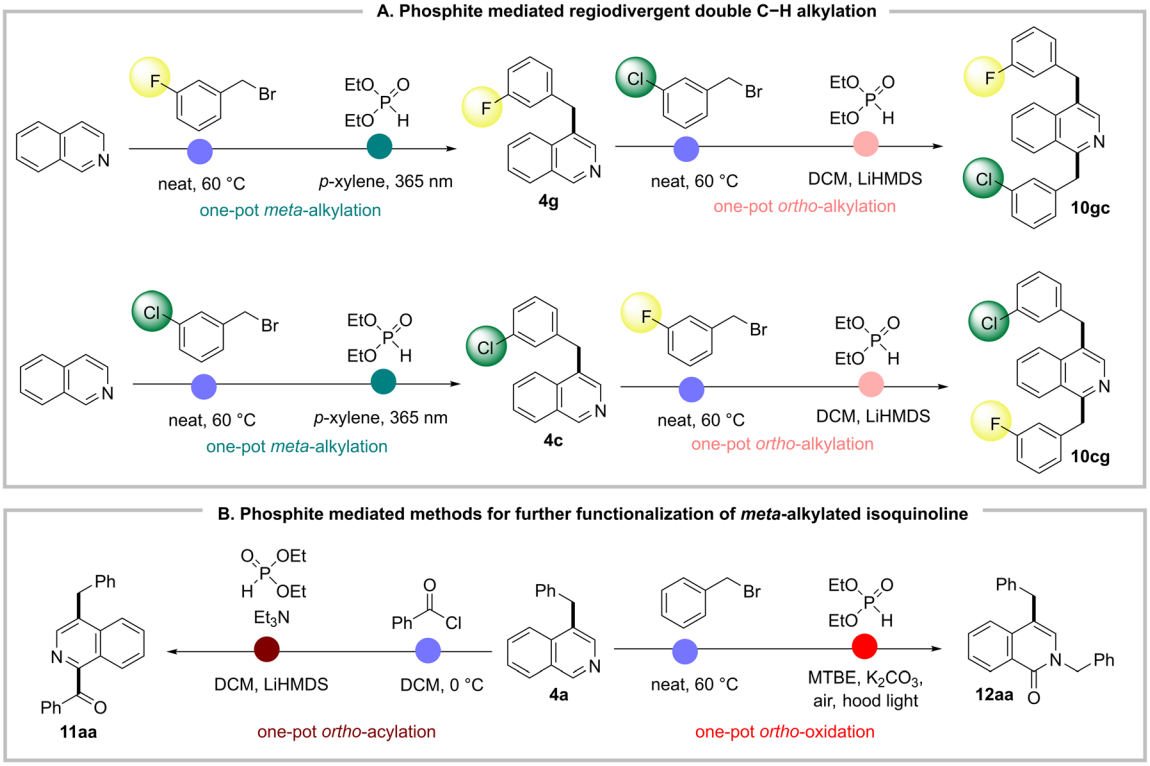

Fig. 4 Molecular editing of isoquinoline C–H bonds *via* sequential *N*-functionalization and phosphite-mediated migration.

a base-mediated 1,4-phosphite elimination. We exposed adduct **2a** to 365 nm light without any base to trap intermediate **3a**, but it resulted in very little product formation with no detectable intermediate. Quenching the reaction at different times and the analysis of the crude reaction mixture also failed to detect intermediate **3a** *via* mass or NMR. However, we could isolate around 9–13% of **8a**, which might form *via* aerobic oxidative aromatization of the dihydroisoquinoline intermediate **3a**. To validate this hypothesis, we ran the reaction in the presence of air, and that led to a higher amount of **8a** formation (20%) along with **4a** (Fig. 3H).

Molecular editing *via* phosphite mediated sequential *N*-functionalization and regio-selective C–H functionalization

Sequential and regioselective C–H bond functionalization of isoquinolines is immensely attractive for the derivatization of the bioactive isoquinolines to improve and expand their potential drug candidacy. For example, *ortho*, *meta*-dialkyl isoquinolines are frequently screened for SAR studies in bioactivity assessment.[4c,d,31] The synthesis of these regioselective double alkylated isoquinolines requires multiple steps with different alkylating reagents and catalysts. With our previous *ortho*-alkylation method from the same starting material **1** in hand,[8b] we tested the feasibility of sequential *N*-alkylation and phosphite mediated regioselective rearrangements for multiple C–H alkylations with different alkyl groups regioselectively. In our first sequence, we alkylated the isoquinoline nitrogen with the *meta*-fluoro benzyl group (**1g**) for its photochemical migration to the *meta*-position (**4g**). Subsequently, **4g** nitrogen was alkylated with the *meta*-chloro benzyl group for its *ortho*-alkyl migration method, successfully generating the *ortho*, *meta*-dialkylated product **10gc** with 45% yield. It is significant to note that the benzyl group on nitrogen can selectively migrate to either the *ortho*- or *meta*-position *via* the same phosphite adduct **2**, only by varying basic *vs.* photochemical reaction conditions. To further demonstrate the utility of this consecutive regioselective approach, we reverse the sequence of *N*-alkylation with *meta*-fluoro and *meta*-chlorobenzyl groups. As a result, the regiodivergent dialkyl isoquinoline **10cg** formed successfully with complete regioselectivity. This unprecedented regiodivergency *via* a common phosphite adduct of *N*-alkyl isoquinoline gives us great control in functionalizing multiple C–H bonds to access densely functionalized isoquinolines (Fig. 4A).

To further demonstrate the synthetic utility of the *meta*-alkylated product **4**, we attempted an *N*-acylation and unreported phosphite-mediated migration of an acyl (benzoyl) group to the *ortho*-position.[32] To our delight, the corresponding phosphite adduct underwent base-mediated benzoyl migration to the *ortho*-position smoothly to form *ortho*-acyl-*meta*-alkyl isoquinoline **11aa** with 68% yield. Next, we did *N*-benzylation of **4a**, and the intermediate was oxidized in air *via* another phosphite-mediated method to form *N*-benzylated isoquinolone **12aa** in good yield (Fig. 4B).[14b]

Conclusions

In summary, we have developed a new photochemical method for the migration of an *N*-alkyl group on isoquinoline to its

meta-position. This *meta*-C–H alkylation of isoquinoline works with all primary, secondary, and tertiary alkyl migrating groups to form sterically demanding secondary, tertiary, and all-carbon quaternary substitutions. A variety of functional groups on both migrating carbon and isoquinoline were tolerated. Sequential *N*-alkylation, followed by phosphite-mediated method manipulations, led to double C–H alkylation to regiodivergent *ortho*, *meta*-dialkylation of isoquinoline. Other phosphite-mediated methods were also developed and utilized for further C–H functionalization of *meta*-C–H alkylated products. Both experimental and computational mechanistic studies were conducted to establish a probable reaction mechanism. Currently, we are studying the synthesis of *N*-functionalized azaarenium salts with other functional groups for their *meta*-migration as a general waste-free strategy for *meta*-C–H functionalization of azaarenes.

Data availability

The complete data supporting this article have been uploaded as part of the ESI material.†

Author contributions

S. R. and D. K. D. conducted the experiments and analysed the data for the optimization study, substrate scope synthesis and experimental mechanistic study under the supervision of P. M. M. A. performed the experiments for sequential functionalization of isoquinoline. A. K. R. designed and performed the computational study under the supervision of A. P. N. A. R. P. conducted the NMR study and analysed the data. P. M. and A. P. directed the project and wrote the manuscript. All authors have given approval to the final version of the manuscript.

Conflicts of interest

There are no conflicts of interest to declare.

Acknowledgements

This research was supported by the SERB (CRG/2019/001065 and SCP/2022/000465), Govt. of India. S. R. and A. K. R. thank CSIR, India for their research fellowship. D. K. D. and M. A. thank DST, India for INSPIRE fellowship. We thank Dr Nilofar Baral for her experimental help. The support from the central analytical facility, NCL is greatly acknowledged.

Notes and references

1 (*a*) C. Luo, M. Ampomah-Wireko, H. Wang, C. Wu, Q. Wang, H. Zhang and Y. Cao, *Anti-Cancer Agents Med. Chem.*, 2021, **21**, 811–824; (*b*) K. W. Bentley, *Nat. Prod. Rep.*, 1992, **9**, 365–391; (*c*) M. Chrzanowska and M. D. Rozwadowska, *Chem. Rev.*, 2004, **104**, 3341–3370; (*d*) M. Chrzanowska, A. Grajewska and M. D. Rozwadowska, *Chem. Rev.*, 2016, **116**, 12369–12465; (*e*) A. N. Kim, A. Ngamnithiporn, E. Du and B. M. Stoltz, *Chem. Rev.*, 2023, **123**, 9447–9496.

2 (*a*) C. M. Marshall, J. G. Federice, C. N. Bell, P. B. Cox and J. T. Njardarson, *J. Med. Chem.*, 2024, **67**, 11622–11655; (*b*) E. A. Bakhite, I. S. Marae, M. A. Gad, S. K. Mohamed, J. T. Mague and S. Abuelhassan, *J. Agric. Food Chem.*, 2022, **70**, 9637–9644; (*c*) N. W. Alcock, J. M. Brown and D. I. Hulmes, *Tetrahedron: Asymmetry*, 1993, **4**, 743–756; (*d*) A. Tsuboyama, H. Iwawaki, M. Furugori, T. Mukaide, J. Kamatani, S. Igawa, T. Moriyama, S. Miura, T. Takiguchi, S. Okada, M. Hoshino and K. Ueno, *J. Am. Chem. Soc.*, 2003, **125**, 12971–12979.

3 (*a*) Z. Fan, X. Chen, K. Tanaka, H. S. Park, N. Y. S. Lam, J. J. Wong, K. N. Houk and J.-Q. Yu, *Nature*, 2022, **610**, 87–93; (*b*) C. M. Josephitis, H. M. H. Nguyen and A. McNally, *Chem. Rev.*, 2023, **123**, 7655–7691; (*c*) S. Maity, A. Bera, A. Bhattacharjya and P. Maity, *Org. Biomol. Chem.*, 2023, **21**, 5671–5690.

4 (*a*) V. Palani, C. L. Hugelshofer, I. Kevlishvili, P. Liu and R. Sarpon, *J. Am. Chem. Soc.*, 2019, **141**, 2652–2660; (*b*) D. Bhowmik, F. Buzzetti, G. Fiorillo, F. Orzi, T. M. Syeda, P. Lombardi and G. S. Kumar, *Med. Chem. Commun.*, 2014, **5**, 226–231; (*c*) Q. Zhang, G. Tu, Y. Zhaoa and T. Cheng, *Tetrahedron*, 2002, **58**, 6795–6798; (*d*) R. Nishikawa-Shimono, Y. Sekiguchi, T. Koami, M. Kawamura, D. Wakasugi, K. Watanabe, S. Wakahara, K. Matsumoto and T. Takayama, *Bioorg. Med. Chem. Lett.*, 2012, **22**, 3305–3310; (*e*) J. W. Hernandez, J. Pospech, U. Klöckner, T. W. Bingham and D. Sarlah, *J. Am. Chem. Soc.*, 2017, **139**, 15656–15659.

5 (*a*) F. Minisci, E. Vismara, F. Fontana, G. Morini, M. Serravalle and C. Giordano, *J. Org. Chem.*, 1986, **51**, 4411–4416; (*b*) J. C. Lewis, R. G. Bergman and J. A. Ellman, *J. Am. Chem. Soc.*, 2007, **129**, 5332–5333; (*c*) T. Andou, Y. Saga, H. Komai, S. Matsunaga and M. Kanai, *Angew. Chem., Int. Ed.*, 2013, **52**, 3213–3216.

6 (*a*) H. M. S. Haley, S. E. Payer, S. M. Papidocha, S. Clemens, J. Nyehuis and R. Sarpong, *J. Am. Chem. Soc.*, 2021, **143**, 4732–4740; (*b*) G. Laudadio, P. Neigenfind, A. Peter, C. Z. Rubel, M. A. Emmanuel, M. S. Oderinde, T. E.-H. Ewing, M. D. Palkowitz, J. L. Sloane, K. W. Gillman, D. Ridge, M. D. Mandler, P. N. Bolduc, M. C. Nicastri, B. Zhang, S. Clementson, N. N. Petersen, P. Martin-Gago, P. Mykhailiuk, K. M. Engle and P. S. Baran, *Angew. Chem., Int. Ed.*, 2024, e202314617.

7 (*a*) D. E. Minter and M. A. Re, *J. Org. Chem.*, 1988, **53**, 2653–2655; (*b*) F. Xie, R. Xie, J.-X. Zhang, H.-F. Jiang, L. Du and M. Zhang, *ACS Catal.*, 2017, **7**, 4780–4785; (*c*) Z. Liu, J.-H. He, M. Zhang, Z.-J. Shi, H. Tang, X.-Y. Zhou, J.-J. Tian and X.-C. Wang, *J. Am. Chem. Soc.*, 2022, **144**, 4810–4818; (*d*) Z. Liu, Z.-J. Shi, L. Liu, M. Zhang, M.-C. Zhang, H.-Y. Gou and X.-C. Wang, *J. Am. Chem. Soc.*, 2023, **145**, 11789–11797; (*e*) J.-J. Tian, R.-R. Li, G.-X. Tian and X.-C. Wang, *Angew. Chem., Int. Ed.*, 2023, **62**, e202307697; (*f*) R. Muta, T. Torigoe and Y. Kuninobu, *Org. Lett.*, 2022, **24**, 8218–8222; (*g*) H. Cao, Q. Cheng and A. Studer, *Science*, 2022, **378**, 779–785; (*h*) P. Xu, Z. Wang, S.-M. Guo and A. Studer, *Nat. Commun.*, 2024, **15**, 4121; (*i*) A. J. Day,

T. C. Jenkins, M. Kischkewitz, K. E. Christensen, D. L. Poole and T. J. Donohoe, *Org. Lett.*, 2023, **25**, 614–618.

8 (*a*) A. Motaleb, S. Rani, T. Das, R. G. Gonnade and P. Maity, *Angew. Chem., Int. Ed.*, 2019, **58**, 14104–14109; (*b*) S. Rani, S. R. Dash, A. Bera, M. N. Alam, K. Vanka and P. Maity, *Chem. Sci.*, 2021, **12**, 8996–9003; (*c*) N. Baral, S. Rani, P. Saikia and P. Maity, *Eur. J. Org Chem.*, 2023, **26**, e202201238.

9 (*a*) Y. Nakao, Y. Yamada, N. Kashihara and T. Hiyama, *J. Am. Chem. Soc.*, 2010, **132**, 13666–13668; (*b*) S. Jung, S. Shin, S. Park and S. Hong, *J. Am. Chem. Soc.*, 2020, **142**, 11370–11375; (*c*) W. Lee, S. Jung, M. Kim and S. Hong, *J. Am. Chem. Soc.*, 2021, **143**, 3003–3012; (*d*) J. Choi, G. Laudadio, E. Godineau and P. S. Baran, *J. Am. Chem. Soc.*, 2021, **143**, 11927–11933; (*e*) S. Jung, H. Lee, Y. Moon, H.-Y. Jung and S. Hong, *ACS Catal.*, 2019, **9**, 9891–9896; (*f*) Y. Gu, Y. Shen, C. Zarate and R. Martin, *J. Am. Chem. Soc.*, 2019, **141**, 127–132; (*g*) T. Nishida, H. Ida, Y. Kuninobu and M. Kanai, *Nat. Commun.*, 2014, **5**, 3387–3392; (*h*) M. Jaric, B. A. Haag, A. Unsinn, K. Karaghiosoff and P. Knochel, *Angew. Chem., Int. Ed.*, 2010, **49**, 5451–5455.

10 K. Murakami, S. Yamada, T. Kaneda and K. Itami, *Chem. Rev.*, 2017, **117**, 9302–9332.

11 G.-Q. Sun, P. Yu, W. Zhang, W. Zhang, Y. Wang, L.-L. Liao, Z. Zhang, L. Li, Z. Lu, D.-G. Yu and S. Lin, *Nature*, 2023, **615**, 67–72.

12 H. Cao, D. Bhattacharya, Q. Cheng and A. Studer, *J. Am. Chem. Soc.*, 2023, **145**, 15581–15588.

13 S. Alwarsh, Y. Xu, S. Y. Qian and M. C. McIntosh, *Angew. Chem., Int. Ed.*, 2016, **55**, 355–358.

14 (*a*) V. K. Aggarwal, I. Bae, H.-Y. Lee and D. T. Williams, *Angew. Chem., Int. Ed.*, 2003, **42**, 3274–3278; (*b*) A. Motaleb, A. Bera and P. Maity, *Org. Biomol. Chem.*, 2018, **16**, 5081–5085.

15 (*a*) C. G. Nasveschuk and T. Rovis, *Org. Biomol. Chem.*, 2008, **6**, 240–254; (*b*) M. N. Alam, S. R. Dash, A. Mukherjee, S. Pandole, U. K. Marelli, K. Vanka and P. Maity, *Org. Lett.*, 2021, **23**, 890–895.

16 J. W. Lown, M. H. Akhtar and R. S. McDaniel, *J. Org. Chem.*, 1974, **39**, 1988–2006.

17 (*a*) G. Cavallo, P. Metrangolo, R. Milani, T. Pilati, A. Priimagi, G. Resnati and G. Terraneo, *Chem. Rev.*, 2016, **116**, 2478–2601; (*b*) J. C. Koziar and D. O. Cowa, *Acc. Chem. Res.*, 1978, **11**, 334–341; (*c*) Z. He, W. Zhao, J. W. Y. Lam, Q. Peng, H. Ma, G. Liang, Z. Shuai and B. Z. Tang, *Nat. Commun.*, 2017, **8**, 416.

18 T. Fan, Y. Cheng, W. Wei, Q. Zeng, X. Guo, Z. Guo, Y. Li, L. Zhao, Y. Shi, X. Zhang, J. Jiang, Y. Wang, W. Kong and D. Song, *J. Med. Chem.*, 2022, **65**, 7399–7413.

19 (*a*) M. D. P. C. Soriano, N. Shankaraiah and L. S. Santos, *Tetrahedron Lett.*, 2010, **51**, 1770–1773; (*b*) Y. Li and C. D. Smolke, *Nat. Commun.*, 2016, **7**, 12137.

20 J. Zhu and A. J. Bennet, *J. Am. Chem. Soc.*, 1998, **120**, 3887–3893.

21 (*a*) J. Slutsky and H. Kwart, *J. Am. Chem. Soc.*, 1973, **95**, 8678–8685; (*b*) T. Yamabe, K. Nakamura, Y. Shiota, K. Yoshizawa, S. Kawauchi and M. Ishikawa, *J. Am. Chem. Soc.*, 1997, **119**, 807–815; (*c*) N. Hammer, M. L. Christensen, Y. Chen, D. Naharro, F. Liu, K. A. Jørgensen and K. N. Houk, *J. Am. Chem. Soc.*, 2020, **142**, 6030–6035.

22 (*a*) E. R. Wearing, D. E. Blackmun, M. R. Becker and C. S. Schindler, *J. Am. Chem. Soc.*, 2021, **143**, 16235–16242; (*b*) M. R. Gatazka, E. C. McFee, C. H. Ng, E. R. Wearing and C. S. Schindler, *Org. Biomol. Chem.*, 2022, **20**, 9052–9068.

23 (*a*) X. Su, H. Huang, Y. Yuan and Y. Li, *Angew. Chem., Int. Ed.*, 2017, **56**, 1338–1341; (*b*) L. Xie, X. Zhen, S. Huang, X. Su, M. Lin and Y. Li, *Green Chem.*, 2017, **19**, 3530–3534; (*c*) H. Wang, P. Bellotti, X. Zhang, T. O. Paulisch and F. Glorius, *Chem*, 2021, **7**, 3412–3424; (*d*) F. C. S. Silva, K. Doktor and Q. Michaudel, *Org. Lett.*, 2021, **23**, 5271–5276.

24 B. Giese, P. Wettstein, C. Stähelin, F. Barbosa, M. Neuburger, M. Zehnder and P. Wessig, *Angew. Chem., Int. Ed.*, 1999, **38**, 2586–2587.

25 S. Dutta, J. E. Erchinger, F. Strieth-Kalthoff, R. Kleinmans and F. Glorius, *Chem. Soc. Rev.*, 2024, **53**, 1068–1089.

26 A. Mavroskoufis, M. Lohani, M. Weber, M. N. Hopkinson and J. P. Gotze, *Chem. Sci.*, 2023, **14**, 4027–4037.

27 M. Baba, *J. Phys. Chem. A*, 2011, **115**, 9514–9519.

28 J. Vijayasundar, V. Subramanian and B. Rajakumar, *Phys. Chem. Chem. Phys.*, 2019, **21**, 438–447.

29 C. Angeli, R. Cimiraglia, S. Evangelisti, T. Leininger and J.-P. Malrieu, *J. Chem. Phys.*, 2001, **114**, 10252–10264.

30 (*a*) V. W. Bowry, J. Lusztyk and K. U. Ingold, *J. Am. Chem. Soc.*, 1991, **113**, 5687–5698; (*b*) A. A. Martin-Esker, C. C. Johnson, J. H. Horner and M. Newcomb, *J. Am. Chem. Soc.*, 1994, **116**, 9174–9181.

31 (*a*) B. M. Trost, C.-I. J. Hung and Z. Jiao, *J. Am. Chem. Soc.*, 2019, **141**, 16085–16092; (*b*) C. Gaoa, Y. Dua, X. Wanga, H. Caoa, B. Linb, Y. Liua and X. Di, *Bioorg. Med. Chem. Lett.*, 2018, **28**, 2265–2269.

32 (*a*) H. W. Gibson, K. K. Brumfield, R. A. Grisle and C. K. F. Hermann, *J. Polym. Sci., Part A:Polym. Chem.*, 2010, **48**, 3856–3867; (*b*) V. Boekelheide and J. Weinstock, *J. Am. Chem. Soc.*, 1952, **74**, 660–663.